Supplemental Material (pdf files)

Supplementary Figure 1 Absorbance and fluorescence spectra (152 Kb)

Supplementary Figure 2 Peptide binding takes place primarily on the cell surface (84 Kb)

Supplementary Figure 3 Open forms of (4-DAPA)- and (4-DMNA)- peptides (268 Kb)

Supplementary Table 1 Binding affinity of fluorogenic peptides (36 Kb)

Supplementary Table 2 (6-DMNA)-RSMA$_4$L fluorescence intensity in different solvents (48 Kb)

Supplementary Table 3 Fluorescence lifetimes for free and DR-bound peptides (76 Kb)

Supplementary Table 4 Data collection and refinement statistics (molecular replacement) (72 Kb)

Supplementary Methods Preparation and analysis of ring open forms; crystal structure; MHC-peptide binding assay; T cell activation; fluorescence lifetime measurement (96 Kb)

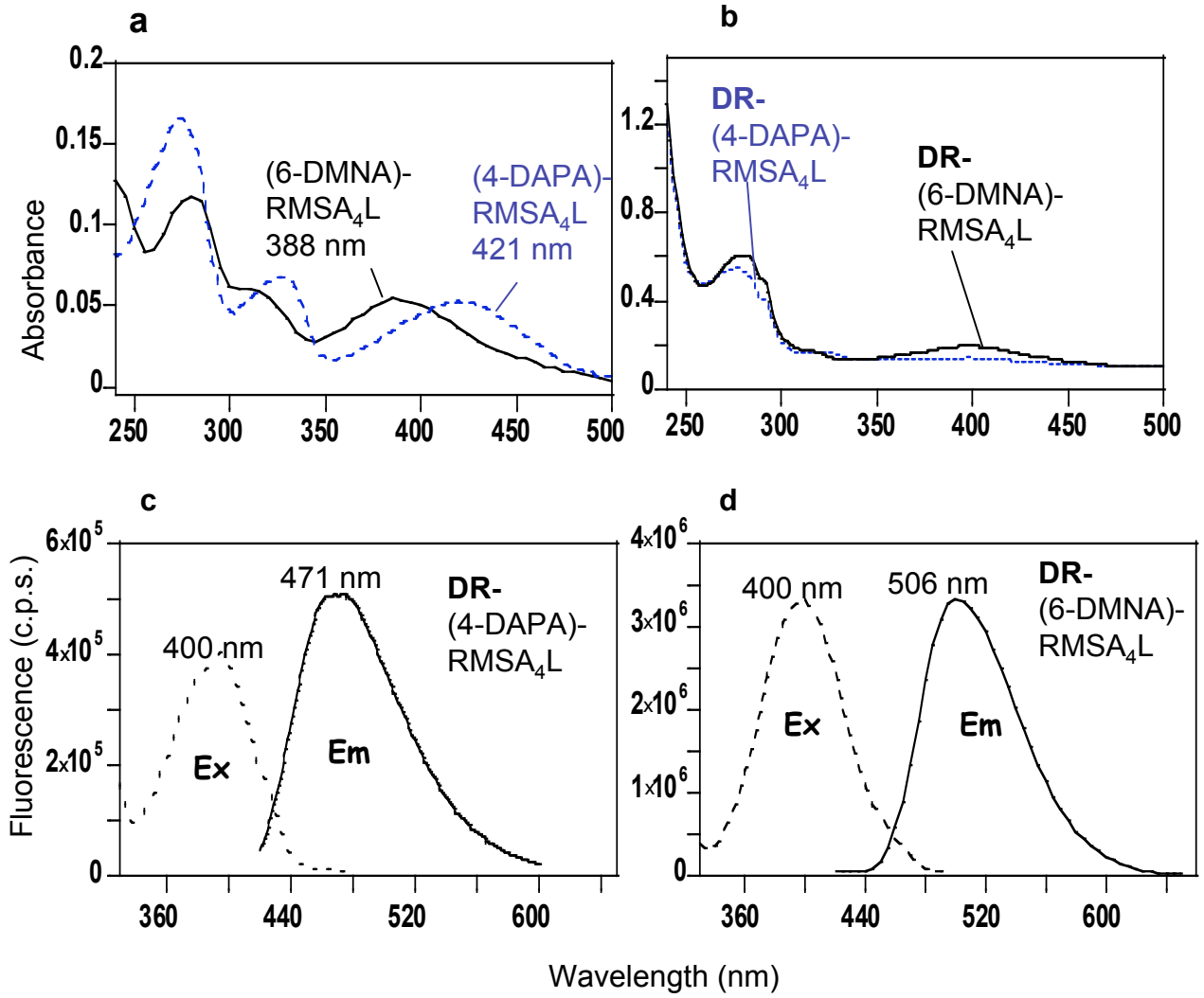

Supplemental Figure 1 Absorbance and Fluorescence Spectra

(**a**) UV-visible spectra of the free peptides. Peptides in a 100 µL volume of PBS pH 7.4 were scanned from 500 – 210 nm using a scan speed of 1 nm/sec (Varian). Molar extinction coefficient of 6480 $M^{-1}cm^{-1}$ for 4-DAPA ($\lambda_{max.em}$ 421nm) and 7980 $M^{-1}cm^{-1}$ for 6-DMNA ($\lambda_{max.em}$ 388nm) were used to estimate the concentration of the free peptides (**b**) Spectra of purified 4-DAPA peptide and 6-DMNA peptide complexes were obtained under similar conditions. Fluorescence excitation and emission spectra of the purified complex (**c** and **d**) were measured as described under methods. Emission scans were performed using 388 nm for the DR (6-DMNA)-RSMAAAAL peptide complex and 421 nm for the (4-DAPA)-RSMAAAAL peptide complex which corresponds to their UV absorption maxima. Excitation scans were obtained using 500 nm emission. The peak intensity for the 4-DAPA peptide-DR1 complex is therefore slightly lower in the excitation scan (471 nm is the λ_{max} of emission).

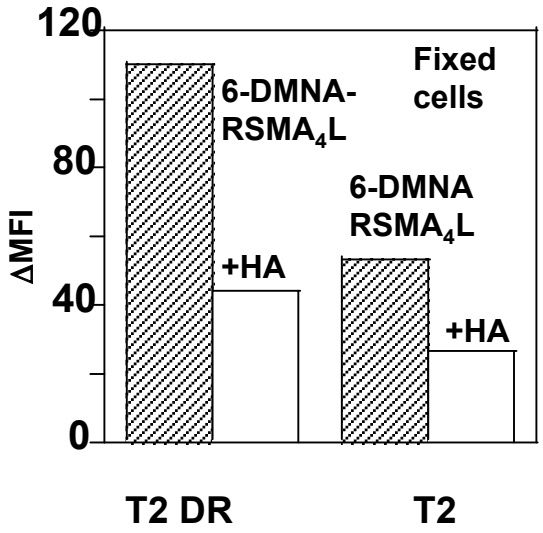

Supplemental Figure 2 Peptide binding takes place primarily on the cell surface

T2 and T2DR cells were fixed in formaldehyde, washed and incubated with the fluorogenic peptide (6-DMNA)-$RSMA_4L$ in the presence or absence of excess unlabelled HA peptide.

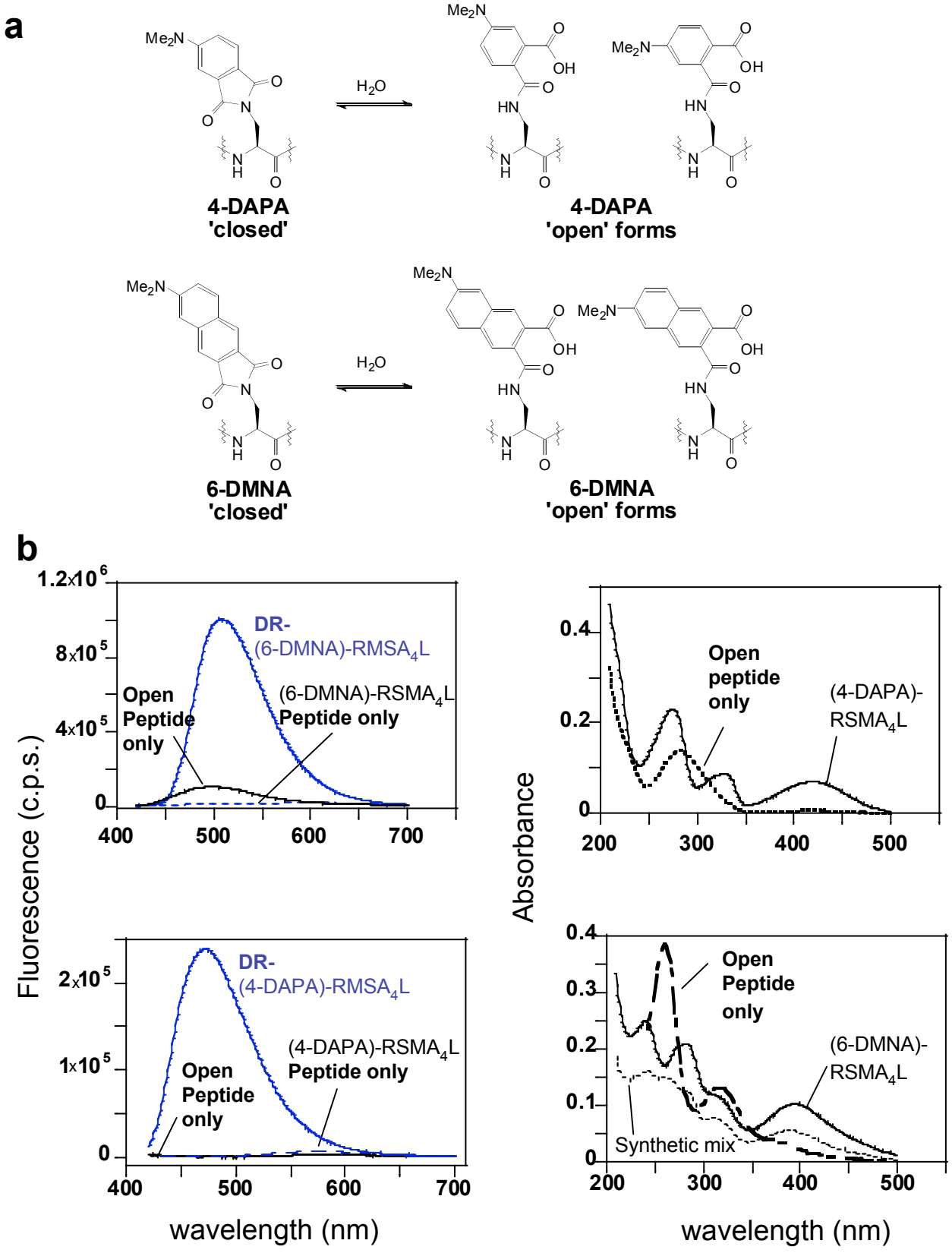

Supplementary Fig 3 (continued on following page)

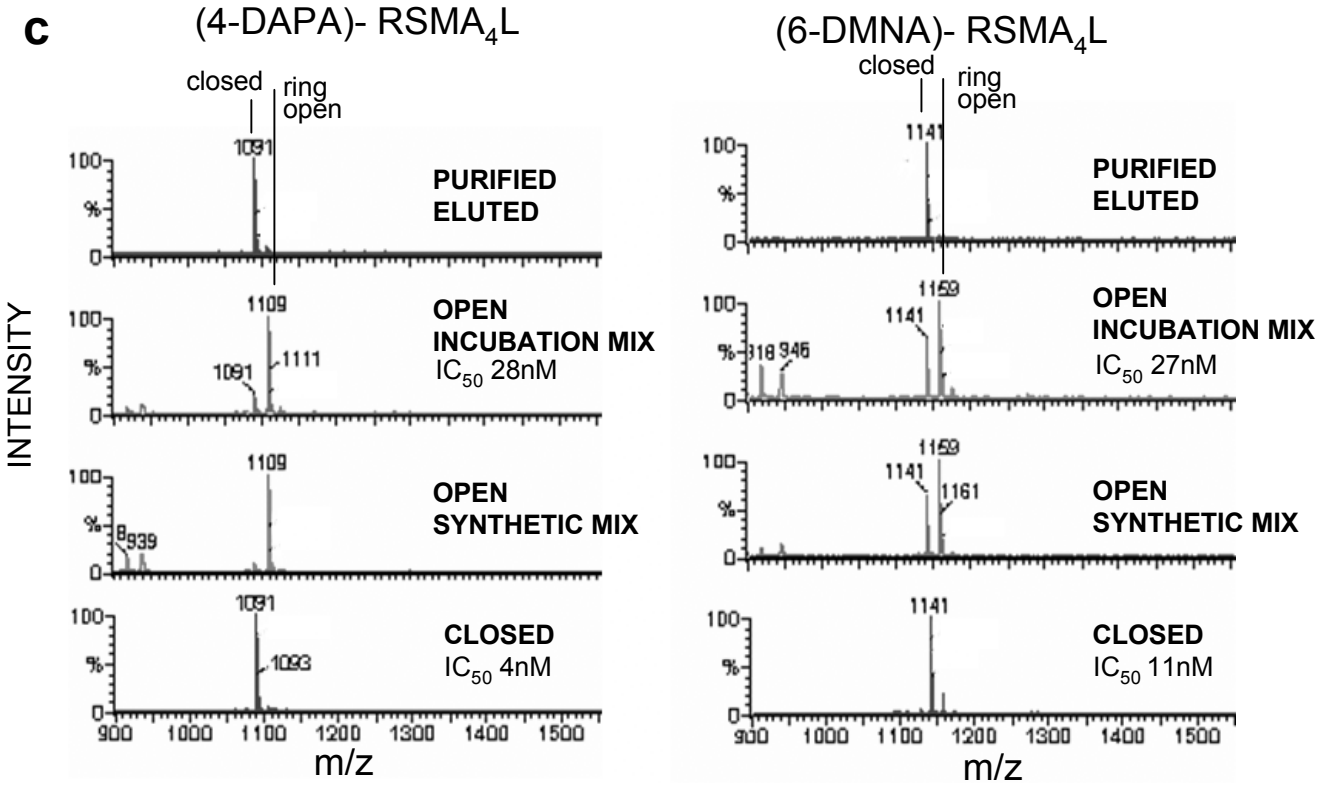

Supplementary Fig 3 Ring-open forms

(**a**) **Structures of the open forms of (4-DAPA)- and (4-DMNA)- peptides.** The fluorophores of the 4-DAPA and 6-DMNA residues undergo spontaneous (reversible) hydrolysis leading to opening of the ring structure.

(**b**) **Spectral properties of the open forms of (6-DMNA)-RSMA$_4$L and (4-DAPA)-RSMA$_4$L.** Fluorescence (left panels) and UV-visible absorbance (right panels) spectra of the synthetic mixtures of purified closed and open forms of (6-DMNA)-RSMA$_4$L (top panels) and of (4-DAPA)-RSMA$_4$L (bottom panels) were measured. Fluorescence spectra of the purified DR peptide complexes derived from the incubation with synthetic mixtures of open and closed forms were simultaneously measured. Note that although the spectral properties of the open (6-DMNA)-RSMA$_4$L peptide is similar to that of the DR1-peptide complex it is ~ 100 fold less fluorescent (**Supplementary Table 1**). The purified DR1-peptide complex from synthetic mixtures is identical to the DR-peptide complex purified from incubations with the pure closed form of the peptides.

(**c**) **Open forms of the fluorogenic peptides are largely excluded from the binding pocket of DR1.** Mass spectra of pure closed (4-DAPA)-RSMA$_4$L and (6-DMNA)- RSMA$_4$L peptides, their synthetic peptide mixture, incubation mixtures of DR+ synthetic peptide mixtures, and the peptide eluted from purified DR bound with the synthetic mixture were obtained by MALDI TOF. The synthetic mixtures were tested for their ability to inhibit the binding of biotin-HA to DR1, with the resultant IC$_{50}$ values shown. In an independent experiment, we also tested the effect of the open and closed peptides after fresh isolation over a reverse phase column using a very shallow gradient (see UV spectra in supplementary Fig 2) The peptides after two day incubation gave a mass corresponding to that of the closed peptide and the IC$_{50}$ values matched those of the closed forms of the peptide (data not shown) indicating that such incubation in the presence of DR1 favors the formation of closed forms of the peptide and that the binding of the open forms is even weaker than suggested by the IC$_{50}$ values.

Supplementary Table 1 Binding affinity of fluorogenic peptides for HLA-DR1

Peptide	IC 50 (nM)
*(6-DMNA)-RSMA$_4$L	11.5 ± 0.5
*(4-DAPA)- RSMA$_4$L	4 ±1
*HA 306-318	4 ±1
HA-(4-DAPA)	0.6
(4-DAPA)-ETDKDKSR	> 10,000
Fmoc-(4-DAPA)	> 10,000

* Average of two independent experiments

Supplementary Table 2 (6-DMNA)-RSMA$_4$L fluorescence intensity in different solvents and bound to HLA-DR1

Solvent	λmax	Relative fluorescence intensity
	(6-DMNA)-RSMA$_4$L	
PBS	617	=1.0
Ethanol	567	76
Isopropanol	564	76
Dimethyl formamide	550	239
Dichloromethane	525	109
DR-(6-DMNA)-RSMA$_4$L	506	1100
	(6-DMNAopen)-RSMA$_4$L	
PBS	498	10

Supplemental Table 3 Fluorescence lifetimes for free and DR-bound peptides

Peptide	Time constant ns	% Fraction	<Lifetime>[1] ns $\tau >= \sum_i \left(\frac{\alpha_i \tau_i}{\sum_j \alpha_j \tau_j} \right) \cdot \tau_i$	<Lifetime>[2] ns $< \tau >= \sum_i \left(\frac{\alpha_i}{\sum_j \alpha_j} \right) \cdot \tau_i$
(6-DMN)-RSMA$_4$L	0.18 1.97 7.8	80 13 6	4.8	0.88
(4-DAPA)-RSMA$_4$L	0.198 1.4 7.7	95 3 1	2.2	0.31
(4-DAPA)-HA	0.2 1.48 7.2	96 3 2	3.0	0.37
DR-peptide complex				
DR-(6-DMN)-RSMA$_4$L	12.4 3.8 0.5	62 11.7 26	11.8	8.3
DR-(4-DAPA)-RSMA$_4$L	11 4 0.82	19.6 47 33	7.3	4.3
DR-(4-DAPA)-HA	13 3.65 0.6	28 48 24	9.7	5.5

[1]Averaging weighted according to the fraction of total photons with lifetime i.
[2]Averaging weighted according to pre-exponential amplitudes (i.e. area under the decay curve)

Supplementary Table 4 Data collection and refinement statistics (molecular replacement)

	DR1:(4-DAPA)-HA:SEC
Data collection	
Space group	R3
Cell dimensions	
a, *b*, *c* (Å)	171.98, 171.98, 121.13
α, β, γ (°)	90, 90, 120
Resolution (Å)	34-2.3 (2.4-2.3) *
R_{sym} or R_{merge}	0.087 (0.363)
$I / \sigma I$	14 (2)
Completeness (%)	100 (99.9)
Redundancy	4.6 (4.4)
Refinement	
Resolution (Å)	34-2.3
No. reflections	282,886
R_{work} / R_{free}	0.203 / 0.224
No. atoms	
Protein	5046
Water	419
B-factors	
Protein	48.3
Water	51.3
R.m.s. deviations	
Bond lengths (Å)	0.007
Bond angles (°)	1.4

*Highest-resolution shell is shown in parentheses.

Supplementary Methods

Preparation and analysis of ring-open forms

Ac-XRSMAAAAL (where X = N-β-allyloxycarbonyl-L-α,β-diaminopropionic acid, fmoc-protected amino acid obtained from Bachem) was synthesized on PAL-PEG-PS resin (0.20 mmol/g) by automated solid phase peptide synthesis (SPPS) on an Applied Biosystems Inc. 431A synthesizer employing standard Fmoc-protected amino acids, 1-hydroxy-1*H*-benzotriazole (HOBt), and 2-(1-*H*-benzotriazol-1-yl)-1,1,3,3-tetramethylaminium hexafluorophosphate (HBTU). The resin was suspended in dry dichloromethane (10 mM in peptide) and a stream of N_2 was bubbled through the solution for 5 minutes. $Pd(PPh_3)_4$ (0.2 equiv.) and phenylsilane (25 equiv.) were then added to the solution which was maintained under N_2 bubbling for another 15 minutes. The resin was then washed with dichloromethane and DMF. The degassing/deprotection cycle was repeated two more times. The resin containing the free amine was reacted with a solution of the anhydride form of the desired fluorophore (4-dimethylaminophthalenedicarboxylic anhydride or 6-(dimethylamino)-2,3-naphthalenedicarboxylic anhydride for 4-DAPA or 6-DMNA respectively, 1 equiv.) and DIPEA (2 equiv.) in NMP (50 mM in peptide). The mixture was allowed to stir for 2-4 hrs. The resin was then washed with DMF and dichloromethane. The peptides were cleaved from the resin using TFA/H_2O/EDT/TIS (94:2.5:2.5:1), triturated in cold ether and purified by reverse phase HPLC with water/acetonitrile containing 0.1% TFA. The identity of the peptides was confirmed by MALDI-TOF (Ac-4-DAPA peptide amide expected mass 1107.55 observed mass 1108.69; Ac-6-DMNA peptide amide expected mass 1157.57 observed mass 1158.65). Peptides were quantified using the molar extinction coefficients of the open forms, 4-DAPA ε_{299} nm = 11569 $M^{-1}.cm^{-1}$, 6-DMNA ε_{318} nm = 8786 $M^{-1}.cm^{-1}$. Of note, partial ring closure was observed when the peptides were stored in water at acidic pH.

Crystal structure

HLA-DR1 extracellular domain was produced by expression of the alpha and beta subunits in *E. coli* followed by in vitro folding, peptide loading, and final isolation by gel filtration, as described[28]. The bacterial superantigen, SEC-3B2, was expressed in folded form in the *E. coli* periplasm and isolated as described[29]. A 1:1 mixture of DR1-(4-DAPA)-HA and SEC-3B2 was crystallized by vapor diffusion against 100 mM sodium acetate, 2% PEG 4K and 10% ethylene glycol at 4^{o}C. A 100 μm cubic crystal was transferred to 25% ethylene glycol v/v in mother liquor and cooled to -190 ^{o}C for data collection at the National Synchrotron Light Source beamline X-25 using 1.1 Å radiation. Diffraction data were processed using HKL2000[30], and phased using a DR1-SEC model from the 2.1 Å crystal structure of another peptide complex (PDB ID 1PYW). Initial unrefined omit maps exhibited clear density for the 4-DAPA side chain that extended only to the middle of the aryl ring, and smeared density for the Pheβ89 side chain. The model excluding 4-DAPA and Pheβ89 was improved by several cycles of manual rebuilding, automated refinement using Refmac and TLS [31] or CNS[32], and addition of ordered water molecules. Omit maps from the improved models exhibited improved 4-DAPA and Pheβ89 side-chain density. The 4-DAPA topological parameters and refinement restraints were obtained from the PRODRG server[33], and were used to include 4-DAPA in the model. Examination of positive and negative electron density in Fobs-Fcalc difference maps suggested a possible minor alternate orientation of the 4-DAPA ring corresponding to a χ_2 rotation of ~180º (as originally modeled, see Figure 1), with a corresponding motion of Pheβ89. However, inclusion of this alternate conformation at various occupancy levels did not improve the refinement statistics or appearance of the electron density, therefore it was not included in the

final model. Data collection and refinement statistics are shown in Table II. Coordinates for this model have been deposited with the PDB and will be available with ID 2IPK.

MHC-peptide binding assay

Peptide binding affinity was measured using a competition assay, as previously described[27]. Briefly, 20 nM of HLA-DR1 was incubated with 20 nM of biotin-HA (K_d ~ 14 nM), in the presence of various concentrations of competitor peptide in PBS + 0.01% Tween 20 for 3 days at 37 ^{0}C. DR1-biotinHA complexes were then quantified using a sandwich ELISA, with immobilized anti-DR capture antibody LB3.1 and streptavidin-alkaline phosphatase detection system. Competition curves were fit to a four-parameter equation for estimation of the IC_{50} value.

T cell activation

A murine T cell hybridoma carrying the HLA-DR1-restricted HA[316-318] peptide-specific T cell receptor HA1.7 and human CD4, a kind gift of Jerome Bill (Univ. Colorado Health Sciences Center), was used to evaluate the biological activity of the modified HA peptide. HLA-DR1+ B-lymphoblastoid LG-2 cells (20,000 per well in 0.1 mL) were pulsed (in triplicate) with the indicated concentration of peptide for 3.5 hours at 37 ^{0}C, 5% CO_2 in RPMI medium supplemented with 10% FBS. After incubation the cells were washed 5 times with fresh medium, and then 10,000 T cells were added in the same medium for an additional incubation of 24 hours under the same conditions as above. Supernatants were removed and assayed for secreted IL-2 using the IL-2 dependent cell line CTLL-2 and a ^{3}H-thymidine incorporation assay.

Fluorescence lifetime measurement

For fluorescence lifetime measurement of the complex, time-correlated single-photon measurements were taken using an in-house apparatus which utilizes the doubled output of a Ti:Sapphire laser (Coherent Mira900D). Purified DR-(6-DMNA)-$RSMA_4L$ (0.35 μM), (6-DMNA)-$RSMA_4L$ alone (0.43 μM), purified DR-(4-DAPA)-$RSMA_4L$ (1 μM), (4-DAPA)-$RSMA_4L$ alone(1.33 μM), purified DR-(4-DAPA)-HA (0.5 μM), and (4-DAPA)-HA alone, were analyzed at the concentrations indicated in parentheses in PBS pH 7.4 in a total volume of 150 μL. Measurements were made at 20 ^{0}C using ~ 13 nM band width, 390 nm monochromatic excitation and 520 nm emission with a pulse repetition rate of 3.8 MHz, with the resultant curves fit to multiexponential decay equations with iterative deconvolution of the instrument response (~60 ps or ~200 ps full-width at half-maximum).